Thermodynamic and Conformational Changes upon Stretching a Poly(dimethylsiloxane) Chain in the Melt

James S. Smith,* Dmitry Bedrov, and Grant D. Smith

Department of Materials Science and Engineering and Department of Chemical Engineering, University of Utah, 122 S. Central Campus Dr., Room 304, Salt Lake City, Utah 84112

Edward M. Kober

Theoretical Division, Los Alamos National Laboratory, Los Alamos, New Mexico 87545

Received April 12, 2005; Revised Manuscript Received June 27, 2005

ABSTRACT: Molecular dynamics simulations using umbrella sampling methods to sample the free energy of stretching a poly(dimethylsiloxane) (PDMS) oligomer (M_w = 904 g/mol) in a melt of PDMS oligomers were performed at 300 K. The free energy of stretching and restoring force were found to be mainly a result of the changes in entropy of the chain as the chain was contracted or stretched, and only at severe extensions do energetic contributions due to deformation of internal bends make a significant contribution to the free energy. The changes in entropy with chain extension were found to be due to restrictions in the polymer dihedral sequences, where the average torsional distribution did not change appreciably until severe extensions. Because the PDMS chain studied is only between 3 and 4 statistical segments in length, the force and free energy could not be fit with the exact solutions of the Gaussian or freely jointed chain models over the region of moderate to high stretching, but the wormlike chain model fit well with deviations only at severe extensions. Excellent agreement, even at severe extensions, was achieved using an extensible wormlike chain model wherein the changes in the chain length smaller than the persistence length (determined from the simulations) were used to adjust the end-to-end distances of the chain. Results are compared with previous PDMS stretching simulations in the literature.

I. Introduction

Whether chains link two junction points in a network or bridge between particle surfaces the stretching of individual chains is fundamental to our understanding of polymer rubber elastic behavior.[1,2] Single chain models such as the Gaussian, freely jointed, and wormlike chain models have been used to calculate the dimensions of unperturbed chains as well as the changes in free energy and forces due to stretching.[3] Efforts by experimentalists using atomic force microscopes (AFM) to pull polymer chains with one end anchored or adsorbed to a surface have been successful in measuring the force−extension curves, characteristic segment lengths, and the effects of solvents on systems such as poly(ethylene oxide) (PEO),[4] poly(methacrylic acid) (PMAA),[5] poly(dimethylsiloxane) (PDMS),[6] and biological macromolecules such as proteins and DNA.[7,8] Computer simulations involving the stretching of alkanes,[9] PEO chains in solutions,[10] unfolding proteins,[11] stretching of PDMS chains in networks,[12] and pulling adsorbed PDMS chains off silica surfaces have been performed.[13] In our earlier work on stretching PEO,[10] simulations were in quantitative agreement with experimental measurements of the restoring force as a function of chain extension. This response was different for hydrophobic and hydrophilic solvents, and the detailed molecular mechanisms based upon the polymer conformations and polar solvent interactions were able to explain these differences.[10]

PDMS is an important commercial elastomer used in industries as diverse as home construction, medical appliances, and aerospace, and because of its utility, this polymer has been widely studied. Another reason PDMS elastomers have been heavily investigated is because they make good model networks due to the large amount of available information about their structure, physical properties, and synthesis.[14] The structure of PDMS is unique in that the lability of the Si−O−Si bond and the low conformational relative free energy barriers give it a great deal of dynamic flexibility, which in turn contributes to its unique physical properties such as its low glass transition and viscosity.[15] In addition to the unique physical properties of PDMS melts and networks, PDMS-based polymer nanocomposites exhibit interesting nonlinear viscoelastic behavior which investigators speculate is related to the stretching and slipping of chains forming loops and tails at particle surfaces and perhaps bridges between nanoparticles.[13,16]

Investigators have simulated the force required to pull a single adsorbed chain of PDMS off of a silica surface and to stretch a similar chain in a vacuum.[13] These forces were used to develop an empirical model which accurately predicted the experimental stress associated with stretching a PDMS/silica nanocomposite. The investigators justified using a constant restoring force in the model by assuming that the change in potential energy was roughly linear as a function of the end-to-end stretching distance of the chain and disrupted intramolecular interactions.[13] Experimentalists pulling PDMS chains from a silica surface in heptane using an AFM tip showed that the restoring force is not constant but actually linear with extension for moderate extensions and becomes nonlinear at high extensions in agreement with the freely jointed and wormlike chain models.[6] The agreement between the force measurements and these chain models indicates that the forces in the PDMS/heptane/silica system are mainly entropic and not enthalpic.

It is evident not only that the interactions between the chain and surface and the intramolecular interac-

10.1021/ma050772l CCC: $30.25
Published on Web 08/18/2005

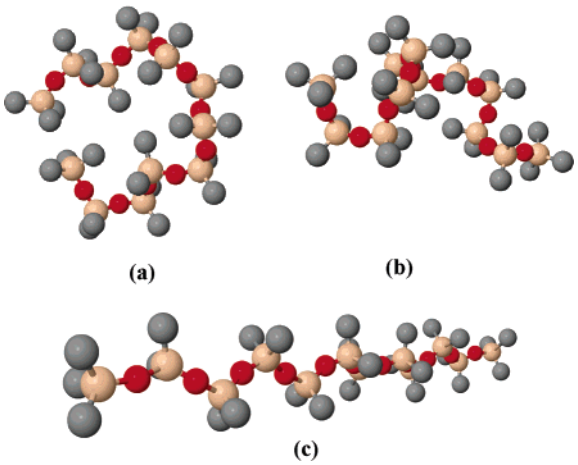

Figure 1. $MD_{10}M$ oligomers: (a) fully contracted to form a loop, (b) near equilibrium ($R = R_{rms}$), and (c) severely stretched ($R/R_{max} = 0.99$). Gray atoms are carbon, red are oxygen, white are silicon, and hydrogen atoms were omitted.

tions within the chain are important but also that the interactions between the chain and surrounding chains or solutions affect its rubber elastic behavior. To better understand the role of conformations and internal structure as well as intermolecular enthalpic and entropic contributions to the free energy of a PDMS chain as a function of extension, we have conducted molecular dynamics (MD) simulations of stretched PDMS oligomers in a PDMS melt at 300 K.

II. Simulation Methodology

As described in our previous work,[10] we can determine the free energy of PDMS chains as a function of end-to-end distance R using the end-to-end distribution function, $W(R)$, obtained from molecular dynamics simulations. Typically $W(R)$ is very hard to determine over a wide range of R due to the low probability of finding chains in the melt in either extremely extended or contracted (loop) configurations. To overcome this difficulty, we used umbrella sampling to obtain $W(R)$ (unbiased) from several biased MD simulations. Throughout this paper and its figures a shorthand notation is used where trimethylsiloxy− ($(CH_3)_3SiO-$) monofunctional units are represented by the letter M and the dimethylsiloxy− ($-(CH_3)_2SiO-$) difunctional units by the letter D with the number of repeat units in subscript.[17] A single $MD_{10}M$ (10 repeat units with molecular weight, M_w = 904 g/mol; see Figure 1) chain in a polymer melt of 39 $MD_{19}M$ chains (19 repeat units, M_w = 1571 g/mol) was biased (stretched or contracted) by a harmonic spring connecting the silicon atoms of its end groups to sample an umbrella or window of end-to-end distances around the predefined distance R_0. The biasing energy of this harmonic spring was $U_s = k_s(R - R_0)^2$, where $k_s = 2.0$ kcal/(mol Å^2) is the force constant used in all the simulations and distances from 4 to 26 Å at 1 Å intervals and from 26 to 36 Å at 2 Å intervals were used for R_0 in order to ensure sufficient umbrella overlap. The self-consistent multiple histogram method was used to recover the unbiased distribution $W(R)$ over the entire range of chain extensions.[18]

All MD simulations were carried out using the Lucretius MD simulation package[19] using a Nosé-Hoover thermostat[20] and barostat[21] to control the temperature and pressure. Bond lengths were constrained using the SHAKE algorithm.[22] The particle mesh Ewald (PME) technique[23] was used to treat all electrostatic interactions. A multiple time step reversible reference system propagator algorithm[24] was used for all NVT production runs with a time step of 0.5 fs for bond, bend, and torsional motions, a 1.0 fs time step for all van der Waals and the real part of the electrostatic interactions within a sphere of radius 7.0 Å, and a 2.0 fs time step for nonbonded interactions in the shell between 7.0 and 10.0 Å and for the reciprocal space PME calculations. Initially the melts were created by replacing one chain in a preequilibrated (over 10 ns) ensemble of 40 $MD_{19}M$ chains with a $MD_{10}M$ chain and continuing NVT production runs for 28 biased umbrellas at the experimental density[25] (0.950 g/cm^3) for an additional 3.0 ns equilibration followed by 5.0 ns of production runs at 300 K, allowing several end-to-end vector relaxations to occur. In all our simulations we used a quantum chemistry-based force field for PDMS.[15]

III. Results and Discussion

Equilibrium and Stretched Chain Dimensions. Chain dimensions such as the mean-squared value of the end-to-end distance, $\langle R^2\rangle_0$, of the unperturbed $MD_{10}M$ chain and total contour length, L_c, at maximum extension are essential to a discussion of the free energy and extension forces of the chain as well as the Gaussian and freely jointed chain models. The value of $\langle R^2\rangle_0$ can easily be determined directly from the MD simulation trajectories. Because the valence angles for alternate backbone bends in PDMS are not equal, the contour length of the chain does not have a precise geometrical description but must be replaced by the maximum end-to-end extension[3] of the chain determined from simulation R_{max}. For the $MD_{10}M$ the values of $\langle R^2\rangle_0 = 280.6$ Å and $R_{max} = 30.5$ Å were used for all necessary calculations. One additional fundamental parameter needed for the freely jointed chain model is the Kuhn length l_k, which is simply the ratio $\langle R^2\rangle_0/R_{max} = 9.2$ Å. The Kuhn length sets the statistical segmental length scale which relates the behavior of the real chain to that of a freely jointed chain of N_k (where $N_k = R_{max}/l_k$ is 3.2) segments with length l_k.[26]

Throughout this work the energies and forces due to changes in the end-to-end distance R are discussed in terms of the dimensionless chain extension ratio R/R_{max}. The unperturbed state end-to-end distance is given by the root-mean-squared value of the end-to-end distance, $R_{rms} = (\langle R^2\rangle_0)^{1/2} = 16.75$ Å, and the region of end-to-end distances below the R_{rms} distance ($R/R_{max} < (R_{rms}/R_{max} = 0.55)$) is referred to as the contracted region, and the end-to-end distances greater than R_{RMS} are referred to as the regions of moderate ($0.55 < R/R_{max} < 0.7$), high ($0.7 < R/R_{max} < 0.9$), and severe ($R/R_{max} > 0.9$) extension.

Free Energy, Restoring Force, Entropy, and Energy for PDMS Chain Extension. From the MD simulations $W(R)$ (Figure 2a) was determined and used to calculate the free energy $A(R)$ (Figure 2a) and force $F(R)$ (Figure 3) as a function of chain extension using the following:

$$A(R) = -k_B T \ln(W(R)) \tag{1}$$

$$F(R) = -\frac{\partial A(R)}{\partial R} = k_B T \frac{\partial \ln(W(R))}{\partial R} \tag{2}$$

where R is the end-to-end distance, k_B is Boltzman's constant, T is the temperature, and $k_B T$ sets the energy scale.

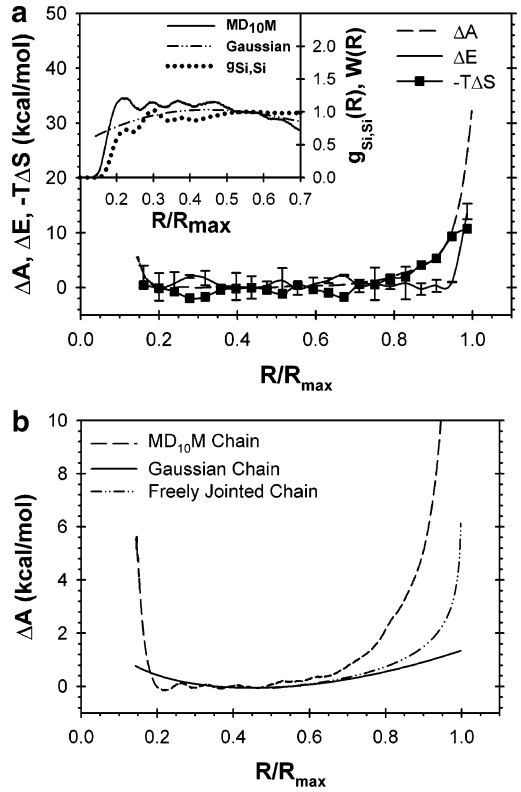

Figure 2. (a) Change in Helmholtz free energy A, system energy E, and entropy $-T\Delta S$, of a $MD_{10}M$ chain stretched in a $MD_{19}M$ chain melt at 300 K. The inset shows a plot of the end-to-end distribution functions, $W(R)$, for the $MD_{10}M$ and Gaussian chains. The two-body intermolecular self-correlation function for silicon is included to show the local packing structure in the melt which affects the contraction and extension of the chains below $R/R_{max} = 0.4$. (b) The free energy of stretching a $MD_{10}M$ chain is compared with the Gaussian and freely jointed chain models (four segments).

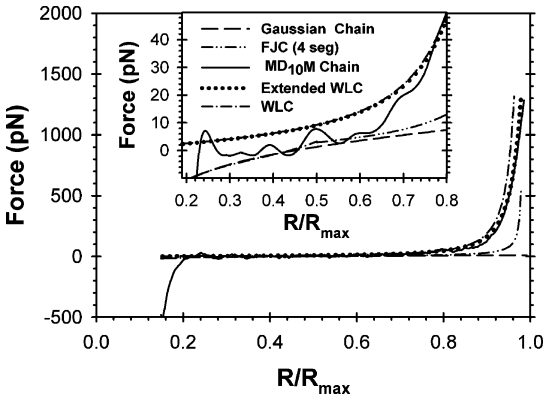

Figure 3. Restoring force as the $MD_{10}M$ is pulled from full contraction to full extension of the chain ends. The inset shows the agreement between the oligomer and Gaussian and freely jointed chain models for contraction and low extensions and the crossover to agreement with the wormlike chain model at high extensions.

a. Free Energy of Extension of a Single Chain. The change in free energy ($\Delta A(R) = A(R) - A(R_{rms})$) from full chain contraction (loop formation see Figure 1a) to severe extension (see Figure 1c) is shown in Figure 2. Zero free energy was chosen to occur at the root-mean-square end-to-end distance. Elongation of the chain end-to-end distance from R_{rms} leads to a monotonic increase in the free energy to maximum extension. In the contracted region, the free energy oscillates close to zero as the chain ends approach one another, leading to a slight minimum at $R/R_{max} = 0.22$. The small oscillations in the free energy and $W(R)$ for $R/R_{max} < 0.4$ are caused by the local packing in the melt as shown in the silicon−silicon intermolecular pair correlation functions of the inset in Figure 2a. The maximum in $W(R)$ at $R/R_{max} = 0.22$ corresponds to the maximum of the first peak in the Si−Si pair distribution function. Below $R/R_{max} = 0.22$ the free energy rises rapidly because attempts to further decrease the end-to-end distance leads to the impingement of the chain end group atoms with a strong corresponding energetic repulsion.

Using the Gaussian end-to-end distance distribution[3] $W(R)$ and eq 1, the change in free energy of stretching a single Gaussian chain relative to that at R_{rms} is given by

$$\Delta A(R) = -k_B T\left(\ln\left(\frac{R^2}{\langle R^2\rangle_0}\right) - \frac{3}{2}\left(\frac{R^2}{\langle R^2\rangle_0} - 1\right)\right) \qquad (3)$$

Similarly, by using $W(R)$ for a four segment freely jointed chain[3] to represent the real $MD_{10}M$ chain ($N_k = 3.2$), the change in free energy for an extended freely jointed chain can be calculated from the following:

$$\Delta A(R) = -k_B T\left(\ln\left(\frac{r}{16 l_k^{\,2}}\right) + 2\ln\left(4 - \frac{R}{l_k}\right)\right) \qquad (4)$$

for $R/R_{max} > 0.5$. Figure 2b shows the change in $A(R)$ for the Gaussian and freely jointed model chains. In the region of high and severe extension ($R/R_{max} > 0.7$) the change in the free energy of the $MD_{10}M$ chain is much more rapid than that predicted for the Gaussian and freely jointed chains, and as expected, the $MD_{10}M$ molecule, which is composed of 3−4 statistical segments, exhibits severe deviations from Gaussian behavior.

b. Energetic and Entropic Contributions to the Free Energy. The energetic contributions to the free energy as a function of end-to-end distance, $\Delta E(R)$, can be straightforwardly obtained from the simulation trajectories (Figure 2a). $\Delta E(R)$ is given as the change in the bonded and nonbonded potential energies of all the chains in the simulation as the $MD_{10}M$ ends are stretched from full contraction to R_{max}. Within the uncertainty of the simulations the energy of the system is effectively zero for a large range of extensions from contracted to highly extended ($0.22 < R/R_{max} < 0.9$). At shorter extensions, $R/R_{max} < 0.22$, there is a large increase in repulsive energy due to steric crowding of the chain ends, and at severe extensions, $R/R_{max} > 0.9$, there is a large increase in energy due to the distortions of internal bends and torsions as shown in Figure 4.

The entropy contribution, $-T\Delta S(R)$, to the free energy of stretching is determined from the difference between the free energy and potential energy changes ($-T\Delta S(R) = \Delta A(R) - \Delta E(R)$) shown in Figure 2a. The entropy change is insignificant below R_{rms}, but the decrease in entropy is largely responsible for the additional free energy in the system at higher extensions with no significant energy changes due to the internal bonded degrees of freedom until the chain is severely stretched $R/R_{max} > 0.9$ (Figure 4).

c. Restoring Force of a Single Stretched Chain. The free energy and subsequently the restoring force can be understood in terms of the entropy and energetic contributions. The restoring force as a function of chain

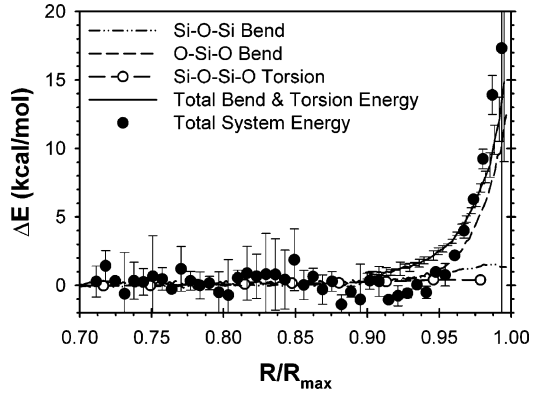

Figure 4. Energy contributed to the free energy of the system due to the deformations of the Si−O−Si and O−Si−O angles, torsional rotations, and sum of all three during stretching at 300 K. The change in the total system energy in high and severe stretching regions is included for comparison.

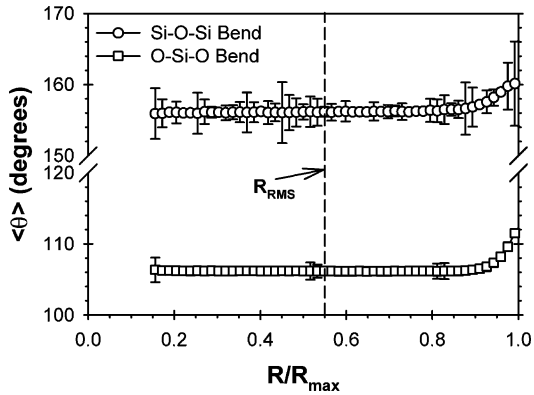

Figure 5. Change in average Si−O−Si and O−Si−O angles from full contraction to severe extension of the chain ends.

extension for the $MD_{10}M$, Gaussian, and freely jointed chains is shown in Figure 3. The restoring force on the chain ends is negative when the chain is fully contracted, indicating that the system is trying to push the ends apart due to the repulsive energy of steric crowding, but from $0.22 < R/R_{max} < 0.70$ as shown in the inset of Figure 3, the force follows the behavior of a Gaussian chain, confirming that it is mainly entropic in this region. The force in part of the contracted region ($0.22 < R/R_{max} < 0.4$) remains positive with a peak at $R/R_{max} = 0.24$ due to the force required for the chain ends to move through the local packing structure (see inset Figure 2a). In the high extension region the increasing forces are mainly due to entropic effects which cannot be represented by the Gaussian and freely jointed chain models, and at severe extensions the rapidly increasing positive force is due to a combination of the entropic effects and strong drive of the bends and constrained torsions to shrink the end-to-end distance of the chain in order to relieve their distortion energy. It is apparent that an analysis of the internal degrees of freedom of the $MD_{10}M$ chain is necessary to explain the energetic and entropic effects responsible for the chain's force−extension behavior at high and severe extensions ($R/R_{max} > 0.6$).

Changes in Local Geometry as a Result of Chain Extension. The largest change in internal energy comes from the stretching of the Si−O−Si and O−Si−O bend angles in the severe stretching regime $R/R_{max} > 0.9$ as shown in Figure 4. Figure 5 shows that the labile Si−O−Si angle deforms in the severely stretched region

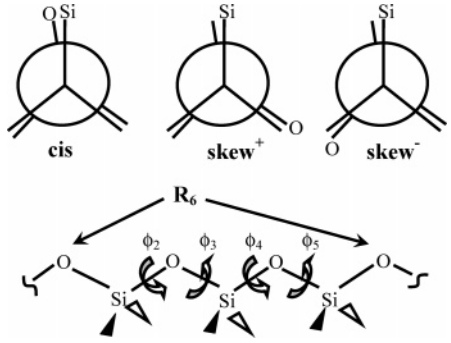

Figure 6. Newman projections of the cis, skew$^+$, and skew$^-$ states of the Si−O−Si−O conformers used to describe the dihedral states in this paper (unlabeled bonds are methyl groups). Also shown is an illustration of the set of dihedrals (ϕ_2, ϕ_3, ϕ_4, and ϕ_5) responsible for the distance, R_6, between two atoms separated by six bonds.

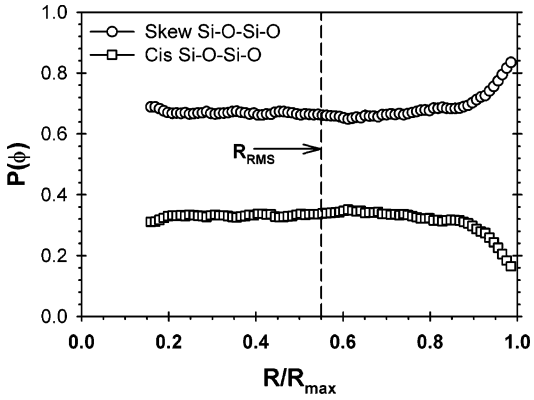

Figure 7. Change in torsion populations for the cis ($\phi = 0 \pm 60°$) and skew ($\phi = \pm 120 \pm 60°$) states from full contraction to maximum extension at 300 K. Note that due to the degeneracy of the skew state, its probability at R_{rms} is twice that of the cis state.

where the average angle increases from 156° to 161° but as shown in Figure 4 contributes little energy to the system due to the low energetic barrier to linearization.[15] The average O−Si−O bend angle also remains unperturbed in Figure 5 until the chain is severely extended $R/R_{max} > 0.9$ where the average angle increases from 105.5° to 111.5°, which triggers a rapid and appreciable change in energy (Figure 4) compared to the Si−O−Si angle energy (approximately 10−12 and 1.8 kcal/mol at R_{max}, respectively).

In our previous work[15] we demonstrated that the relative free energy barriers for individual PDMS backbone torsions and bends are low (~0.1 kcal/mol), which is responsible for the low viscosity and self-diffusion coefficient of the polymer. These low barriers also limit the total energy due to local conformational changes as shown in Figure 4. For the Si−O−Si−O backbone torsion analysis we have defined the following three states: cis (cis = 0 ± 60°, skew$^+$ ($s^+ = 120 \pm 60°$), and skew$^-$ ($s^- = -120 \pm 60°$). For the Si−O−Si−O type torsion the cis, s^+, and s^- states are all eclipsed and differ only by the alignment of the near silicon atom with the far oxygen and methyl groups as shown in Figure 6. Figure 7 shows that the backbone Si−O−Si−O torsion angles for the contracted, moderate, and much of the high extension regimes have a meltlike distribution with the cis and skew populations all about equal (the skew population is twice that of cis because of degeneracy) and relatively flat because of the low PDMS

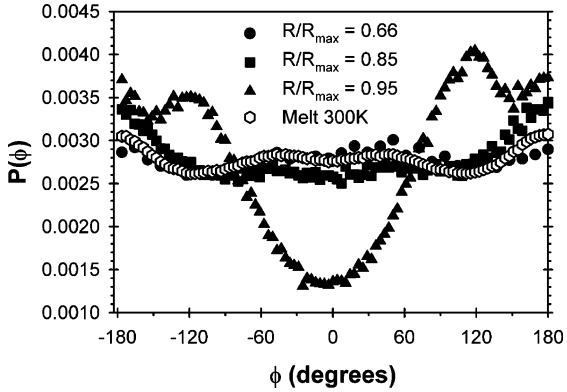

Figure 8. Torsion populations for an $MD_{10}M$ melt and a single chain at biased end-to-end distances R/R_{max}, ranging from moderate ($R/R_{max} = 0.66$) to severe extension ($R/R_{max} = 0.95$) in this work.

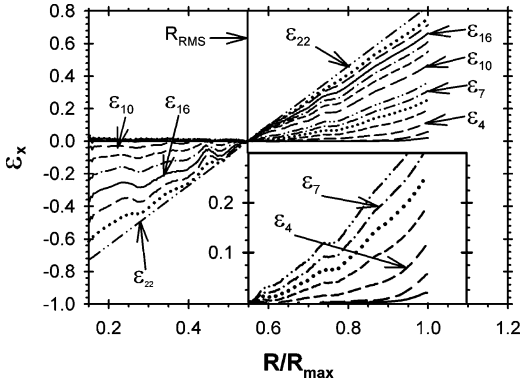

Figure 9. Strain of different segments of the chain as a function of overall chain extension ratio R/R_{max} stretched from full contraction of the ends to maximum extension at 300 K. Inset magnifies the strain for segments separated by x bonds ($x = 2-8$) for chain extension from R_{rms} to R_{max}.

torsional barriers. In the regions of high and severe extension the populations of both torsion states change as the conformations are constrained by the chain stretching. This change is confirmed in Figure 8 where the cis state nearly disappears, and the skew states increase in population when compared to the melt or moderate extension regime. Even in the severe extension region where conformational populations are strongly perturbed, dihedrals make little contribution to the increase in energy with extension, as can be seen in Figure 4, because of the extremely flat conformational energy surface for PDMS.[15] The combined change in backbone bend and torsion energy accounts for most of the total change in system energy as shown in Figure 4. Therefore, there is little change in the total nonbonded energy of the system with chain extension up to the extreme limits of extension.

Contribution of Conformational Changes to the Free Energy. It is clear from Figure 7 that conformational populations do not change significantly until the severe extension region. However, the entropy is increasing even at moderate chain extensions due to configurational restrictions where the actual sequence of dihedral states change without significantly influencing the average conformer populations until severe extensions. To determine on what length scales significant chain perturbations are occurring across the range of contraction and extension, we calculate the distance R_x between any two atoms, A_i and A_{i-x}, in the chain backbone separated by x bonds from MD simulation trajectories. This distance is determined by one set of parameters, the dihedral angles $\{\phi_{i-2}, \phi_{i-3}, ..., \phi_{i-(x+1)}\}$ around the bonds between atoms A_{i-1} and $A_{i-(x+1)}$ assuming that the bend and bond geometries are fixed (see Figure 6).[27] The average segmental end-to-end distance $\langle R_x \rangle$ can be used to calculate the average strain on the segment, ϵ_x, at extension ration R/R_{max} by the following:

$$\epsilon_x(R/R_{max}) = \frac{(\langle R_x(R/R_{max})\rangle - \langle R_x^0\rangle)}{\langle R_x^0\rangle} \tag{5}$$

where $\langle R_x^0 \rangle$ is the average segmental end-to-end distance in the unperturbed chain with end-to-end distance R_{rms}. Figure 9 shows the segmental strain as a function of overall chain extension. We see that in the contracted regions ($R < R_{rms}$) only the end-to-end chain segments longer than nine bonds ($x \geq 9$) where $\langle R_9^0 \rangle = 9.3$ Å are affected by the bending of the chain which agrees well with the Kuhn segment length of the chain, 9.2 Å, calculated in section IIIa.

In the inset of Figure 9 we can see that ϵ_3, which corresponds to individual torsions, does not contribute to the overall chain stretch until $R/R_{max} > 0.85$ in agreement with the conformational changes in Figure 7. For larger segments the changes in segment strain, $\epsilon_4, \epsilon_5, ..., \epsilon_n$, happen immediately upon stretching for $R > R_{rms}$. Once again the deformation of chain segments smaller than l_k occurs without significantly perturbing the conformational populations and is due to restriction of the dihedral sequences that reduces the number of chain configurations and increases the entropy which effectively stiffens the $MD_{10}M$ chain.

Force−Extension Behavior. a. Comparison with Gaussian, Freely Jointed, and Wormlike Model Chains. Using the Gaussian model equation for the change in free energy (eq 3) and relation of eq 2, the restoring force−extension relationship for the Gaussian model is given by the following:

$$F(R) = k_B T\left[\frac{2}{R} - \frac{3R}{\langle R^2\rangle_0}\right] \tag{6}$$

Similarly using eqs 2 and 4, the force−extension of the freely jointed chain model is

$$F(R) = k_B T\left[\frac{1}{R} - \frac{2}{(4l_k - R)}\right] \tag{7}$$

where l_k is the length of a Kuhn segment of the $MD_{10}M$ chain. Equation 7 is valid for a freely jointed chain with four Kuhn segments and at extensions where $R/R_{max} > 0.5$ as discussed in section IIIb.1. At smaller end-to-end distances the forces of the freely jointed chain model coincide with the Gaussian model.[3]

The restoring force as a function of chain extension for the $MD_{10}M$, Gaussian, and freely jointed chains is shown in Figure 3. The failure of the Gaussian chain to model the real chain force−extension curve of real polymers at high extensions in Figure 3 is due to its assumption of infinite extensibility. As shown in the inset of Figure 9 for any extension R/R_{max} greater than 0.65 the average strain in chain segments smaller than the Kuhn length (l_k) becomes significant. The onset of deformation on scales smaller than l_k signifies a breakdown of the freely jointed chain model which causes the

force−extension curve in Figure 3 to cross over from the freely jointed to the wormlike chain model for $R/R_{max} > 0.65$.

The force−extension response of real chains is stiffened by intramolecular flexibility mechanisms[28] such as bending energy or restrictions in conformational sequences on the sub-l_k scale. The restoring force as a function of chain extension for the $MD_{10}M$ chain can be better described at high extensions by the wormlike chain (WLC) model (Figure 3). In the WLC model the governing parameters are the persistence length, L_p, and contour length, L_c, of the chain. The persistence length defines both the scale of correlations between segments of the polymer and extent of any bending fluctuations due to the effective "bending elasticity" of the macromolecule.[28]

As discussed previously (section IIIa) the value of R_{max} is used instead of L_c even though it is typically much less than maximum possible chain length, nl, due to the valence restrictions of the real chain. To determine the value of the persistence length, L_p, we choose a value that forces a correspondence between the characteristic ratio of the model and the real chain:[3]

$$C_\infty \equiv \left(\frac{R_{max}}{nl}\right)\left(\frac{2L_p}{l}\right) \tag{8}$$

where C_∞ for PDMS chains was determined from previous simulations to be 5.5,[15] and $n = 22$ is the number of backbone bonds of length $l = 1.65$ Å. Therefore, the maximum extension and persistence lengths for the $MD_{10}M$ chain in this simulation are 30.5 and 5.4 Å, respectively.

These parameters can be used in the closed form WLC solution[29] to calculate the force $F(R)$ required to extend the chain to an end-to-end distance, R:

$$F(R) = \frac{k_B T}{L_p}\left(\frac{1}{4(1 - R/R_{max})^2} - \frac{1}{4} + \frac{R}{R_{max}}\right) \tag{9}$$

This force−extension relation for the WLC model is an interpolation formula between the analytical solutions at both the small and large force limits and is most accurate at large extensions. It is apparent in the inset of Figure 3 that eq 9 is most effective in describing the simulation force−extension curve at high extensions ($R/R_{max} > 0.7$) and that the $MD_{10}M$ chain crosses over from the Gaussian to the WLC model description at high extension and deviates from the WLC model at severe extensions ($R/R_{max} > 0.85$).

b. Extensible Chain Models. When a chain is severely stretched, elastic extensions of the chains on the scale of the persistence length can lead to equivalent stretching forces being manifest at larger end-to-end separations than the WLC would predict. Several models have been proposed to describe this behavior including the extensible WLC[30,31] and simple harmonic chain models[32] whose corrections are based upon either a f/K_0 correction where K_0 is estimated by the bulk elastic modulus of the material, harmonic bond fluctuations with a bond constant k, or determined empirically by using an additional segmental spring constant to fit the data of single chain stretching experiments.[5] We propose using a methodology wherein the additional elongation is estimated from analyzing the change in separation of atoms whose unperturbed equilibrium separations are near the persistence length L_p (sub-L_p stretching) as the stretching force is applied to the entire chain. The average separation between atoms separated by four bonds, $\langle R_4 \rangle$, was calculated as 4.93 Å for unperturbed chains, which is close to but smaller than the persistence length. Therefore, for the purposes of analyzing the data in Figure 3, we calculated the average change in atomic separation for atoms separated by four bonds as a function of the force necessary to stretch the chain, $\Delta r(f)$, and found that at the high to severe stretching regime there is a square root dependence on the force f as shown in Figure 10. Using this information, it was possible to adjust the value of R and get an excellent fit for the force−extension curve measured in our simulations by the following:

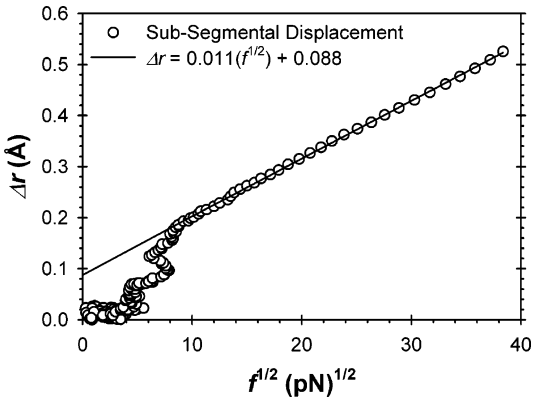

Figure 10. Extension of chain segments shorter than a persistence length, Δr, due to the stretching force applied to the ends of the $MD_{10}M$ chains and results of a linear regression fit at high force.

$$R = R_0 + \Delta r(f) \tag{10}$$

where R_0 was the original end-to-end distance used in eq 9, and a least-squares fit for $\Delta r(f)$ is shown in Figure 10. Figure 3 shows the improved agreement between force−extension curves of the $MD_{10}M$ chain and the WLC model with the corrected end-to-end distance from eq 10. The range of extensions where sub-L_p stretching affects the chain extension coincides with the deformation of the backbone bends and changes in conformational populations shown in Figures 5 and 7 as well as the strains ϵ_2 and ϵ_3 in Figure 9.

Comparison with Previous Work. The change in free energy or restoring force in our work as the chain is stretched is very different from the approximately linear potential energy curves of previous simulations reported in the literature.[13] The PDMS chains they examined were 33−50 repeat units and had initial configurations based upon random torsion assignments followed by a 100 ps minimization of the intramolecular potential in a vacuum (a poor solvent condition). Under such conditions the chain configuration is expected to collapse to maximize the intramolecular nonbonded interactions. They explain the rapid linear rise in potential energy when the chain is stretched as due to the steady pulling of kinks out of the chain in the vacuum and the subsequent changes in intramolecular potential energy after minimization for ~100 ps. These results seem to be in error in assuming that simulations of single chains in a vacuum, where changes in intramolecular energies are very large (many $k_B T$) and dominate entropic changes due to stretching, will correctly capture the entropic and energetic contributions

to the restoring forces of a single stretched chain in a melt or composite.

The stretching simulations in our work are done in a PDMS polymer melt for a long enough time to accumulate sufficient statistics to estimate both the energetic and entropic contributions to the free energy at that extension. Our simulations show that the energetic component of the free energy (Figures 2a and 4) is negligible (within the uncertainty) until the region of severe stretching where it increases until it comprises about half of the free energy. The energy due to distortions of the backbone bends and torsions accounts for the change in system energy as shown in Figure 4. The restoring force in our simulations was approximately linear over a range of extension as predicted by the Gaussian and freely jointed chain models and accurately fit by an extensible WLC model at high and severe extensions. These results agree with experiment, in that the PDMS force−extension curves obtained from experiment[6] also fit the freely jointed chain and WLC models with empirically fit constants at high extensions, showing that the restoring force and free energy are mainly entropic in nature. The conclusion of Hanson[13] that the force of stretching PDMS can be inferred from changes in internal energy is a consequence of simulating in a vacuum and not general to PDMS or other polymer chains in a melt, network, or polymer nanocomposite. Our results demonstrate that surrounding a stretched chain with additional chains is important to accurately represent the restoring force, internal energy, entropy, and change in free energy. These results are also in agreement with the great body of experimental evidence that PDMS deformations are dominated by entropic changes.[14]

IV. Conclusions

The free energy and restoring force of a PDMS chain due to the stretching were calculated from MD umbrella sampling simulations using the self-consistent histogram method. The free energy change was mainly due to the decreasing entropy of the chain as the ends were extended. Additional internal energy due to the distortion of internal bends became significant when the chains were severely stretched. The entropy changes when the $MD_{10}M$ chain is stretched are due to extensions on a range of segmental scales which are caused by restriction of backbone dihedral sequences which decreases the number of configurations without changing the average dihedral populations. The MD simulations showed good agreement between the force−extension relations of $MD_{10}M$ chains and the Gaussian and freely jointed chain model for low to moderated extensions. Further agreement with these models at high extensions was impossible due to the small number of statistical segments and stiffness of the chain, but excellent agreement between the MD simulation results and an extensible WLC model confirmed the entropic nature of the free energy and restoring force in PDMS stretching. The corrections in the extensible WLC model were based on subpersistence length motions due to the change in dihedral populations and deformation of backbone bends and were calculated using the average force−extension behavior of chain segments on the persistence length scale at severe extensions.

Acknowledgment. The authors acknowledge the support of Los Alamos National Laboratory under Contract LANL-0591300104 and thank them for use of their computational facilities for this work.

References and Notes

(1) James, H.; Guth, E. *J. Chem. Phys.* **1943**, *11*, 455−481.
(2) Treloar, L. R. G. In *The Physics of Rubber Elasticity*, 3rd ed.; Oxford: Claredon, 1975.
(3) Flory, P. J. In *Statistical Mechanics of Chain Molecules*; Interscience: New York, 1969.
(4) Osterhelt, F.; Rief, M.; Gaub, H. E. *New J. Phys.* **1999**, *1*, 6.1.
(5) Oritz, C.; Hadziioannou, G. *Macromolecules* **1999**, *32*, 780.
(6) Senden, T. J.; di Meglio, J.-M.; Auroy, P. *Eur. Phys. J. B* **1998**, *3*, 211.
(7) Lavery, R.; Lebrun, A.; Allemand, J.-F.; Bensimon, D.; Croquette, V. *J. Phys.: Condens. Matter* **2002**, *14*, R383.
(8) Bustamante, C.; Bryant, Z.; Smith, S. B. *Nature (London)* **2003**, *421*, 423.
(9) Spitalsky, Z.; Bleha, T. *Macromol. Theory Simul.* **2001**, *10*, 833.
(10) Bedrov, D.; Smith, G. *J. Chem. Phys.* **2003**, *118*, 6656.
(11) Bryant, Z.; Pande, V. S.; Rokhsar, D. S. *Biophys. J.* **2000**, *78*, 584.
(12) Heine, D. R.; Grest, G. S.; Lorenz, C. D.; Tsige, M.; Stevens, M. J. *Macromolecules* **2004**, *37*, 3857.
(13) Hanson, D. E. *J. Chem. Phys.* **2000**, *113*, 7656.
(14) Mark, J. In *Silicon-Based Polymer Science*; Ziegler, J. M., Fearon, F. W. G., Eds.; American Chemical Society: Washington, DC, 1990; p 47. Kuo, A. C. M. In *Polymer Data Handbook*; Mark, J. E., Ed.; Oxford University Press: New York, 1999; pp 411−435. Erman, B.; Mark, J. E. In *Structure and Properties of Rubberlike Networks*; Oxford University Press: New York, 1997; Chapter 9.
(15) Smith, J.; Borodin, O.; Smith, G. *J. Phys. Chem. B* **2004**, *108*, 20340.
(16) Lapra, A.; Clement, F.; Bokobza, L.; Monnerie, L. *Rubber Chem. Technol.* **2003**, *76*, 60.
(17) Hurd, C. B. *J. Am. Chem. Soc.* **1946**, *68*, 364.
(18) Frenkel, D.; Schmidt, B. In *Understanding of Molecular Simulation: From Algorithms to Applications*; Academic: New York, 1996; Chapter 7.
(19) Lucretius http://lucretius.mse.utah.edu/.
(20) Nose, S. In *Computer Simulations in Material Science*; Meyer, M., Pntikis, V., Eds.; Kulwer Academic Publishers: Dordrecht, 1991; p 21.
(21) Maryna, G. J.; Tuckerman, M. E.; Tobias, D. J.; Klein, M. L. *Mol. Phys.* **1996**, *87*, 1117.
(22) Ryckaert, J. P.; Ciccotti, B.; Berendsen, H. J. C. *J. Comput. Chem.* **1977**, *23*, 327.
(23) Deserno, M.; Holm, C. *J. Chem. Phys.* **1998**, *109*, 7678.
(24) Martayna, G. J.; Tuckerman, M.; Berne, B. J. *J. Chem. Phys.* **1992**, *97*, 1990.
(25) Beevers, M. S.; Mumby, S. J.; Clarson, S. J.; Semlyen, J. A. *Polymer* **1983**, *24*, 1565.
(26) Boyd, R. H.; Phillips, P. J. In *The Science of Polymer Molecules*; Cambridge University Press: Cambridge, 1993.
(27) Mattice, W. L.; Suter, U. W. In *Conformational Theory of Large Molecules*; Wiley-Interscience: New York, 1994.
(28) Grosberg, A. Y.; Khokhlov, A. R. In *Statistical Physics of Macromolecules*; AIP Press: New York, 1994.
(29) Bustamante, C.; Marko, J. F.; Siggia, E. D.; Smith, S. *Science* **1994**, *265*, 1599.
(30) Fixman, M.; Kovac, J. *J. Chem. Phys.* **1973**, *58*, 1564.
(31) Odijk, T. *Macromolecules* **1995**, *28*, 7016.
(32) Kierfeld, J.; Niamploy, O.; Sa-yakanit, V.; Lipowsky, R. *Eur. Phys. J. E* **2004**, *14*, 17.

MA050772L